Research Paper https://doi.org/10.7733/jnfcwt.2020.18.3.373

Actinide Drawdown From LiCl-KCl Eutectic Salt via Galvanic/chemical Reactions Using Rare Earth Metals

Dalsung Yoon*, Seungwoo Paek, Jun-Hyuk Jang, Joonbo Shim, and Sung-Jai Lee
Korea Atomic Energy Research Institute, 111, Daedeok-daero 989beon-gil, Yuseong-gu, Daejeon, Republic of Korea

(Received August 27, 2020 / Revised September 14, 2020 / Approved September 18, 2020)

This study proposes a method of separating uranium (U) and minor actinides from rare earth (RE) elements in the LiCl-KCl salt system. Several RE metals were used to reduce UCl_3 and $MgCl_2$ from the eutectic LiCl-KCl salt systems. Five experiments were performed on drawdown U and plutonium (Pu) surrogate elements from $RECl_3$-enriched LiCl-KCl salt systems at 773 K. Via the introduction of RE metals into the salt system, it was observed that the UCl_3 concentration can be lowered below 100 ppm. In addition, UCl_3 was reduced into a powdery form that easily settled at the bottom and was successfully collected by a salt distillation operation. When the RE metals come into contact with a metallic structure, a galvanic interaction occurs dominantly, seemingly accelerating the U recovery reaction. These results elucidate the development of an effective and simple process that selectively removes actinides from electrorefining salt, thus contributing to the minimization of the influx of actinides into the nuclear fuel waste stream.

Keywords: Actinide drawdown, Pyroprocess, Uranium, Electrorefiner, LiCl-KCl

*Corresponding Author.
Dalsung Yoon, Korea Atomic Energy Research Institute, E-mail: dyoon@kaeri.re.kr, Tel: +82-42-868-4802

ORCID

Dalsung Yoon	http://orcid.org/0000-0003-4453-9502	Seungwoo Paek	http://orcid.org/0000-0002-1811-5450
Jun-Hyuk Jang	http://orcid.org/0000-0002-5453-8055	Joonbo Shim	http://orcid.org/0000-0001-8891-2597
Sung-Jai Lee	http://orcid.org/0000-0001-7639-1210		

1. Introduction

Pyroprocessing technology has been regarded as a future technology for the treatment and recycling of used nuclear fuel (UNF) [1-3] owing to its favorable features, such as high proliferation resistance via plutonium (Pu) recovery as a mixture, compact facilities for fuel recovery/fabrication, and rapid on-site support for fast reactor fuel cycle with high radiation stability [4-5]. The electrorefining (ER) process plays a major role in the pyroprocessing technology, i.e., the metallic form of UNF is loaded into an anode basket to be dissolved into LiCl-KCl eutectic salt at 773 K. From the salt, pure uranium (U) is electrochemically collected on a solid cathode while U, Pu, and other minor actinides (MAs) are co-recovered into a liquid cadmium cathode (LCC). After these operations, the remaining salt mostly contains MA and elements in the lanthanide series. Li and co-workers [6] performed LCC electrorefining using a mixed salt from the MK-IV and MK-V electrorefiners, whereby the used metal fuels from Experimental Breeder Reactor-II (EBR-II) faster reactor were processed. They reported that the average concentrations of U, Pu, and rare earth (RE) elements after the LCC runs were 1.34wt%, 1.48wt%, and 4.85wt%, respectively. Therefore, U concentration continuously decreases while MA and RE elements are accumulated via ER operation using the solid and liquid cathodes.

The high concentrations of MA and RE elements in the salt during ER operations would make U separation on the solid cathode inefficient. Therefore, the ER salt needs to be purified periodically, and the MA elements, including Pu, should be separated in advance, in what is typically called an actinide drawdown (DD) process. This process is aimed specifically at the selective recovery of MA from a nuclear fuel waste stream; however, the separation of MAs from RE elements is significantly difficult due to the similarities between thermodynamic and physical properties. Therefore, researchers have studied several methods of separating U and MA from RE elements in the LiCl-KCl salt system. Simpson et al. [7] added metallic lithium (Li) into molten salt to separate RE elements and found that the reaction rate was not correlated to the Gibbs free energy difference. Several studies have focused on separating MA elements using Li alloys, including Li-Cd, Li-Zn, and Li-Bi (reductive extraction) [8-11], whereby the Li-alloy reductants were incrementally added to the salt and the distribution behaviors of the elements were observed. Results of the separation behaviors show that the separation of U and MAs from the RE elements using the liquid metals pools is significantly difficult resulting from that the reduction potentials of the elements become very close.

Shim and co-workers proposed a new approach [12], the use of RE metals as a reductant to remove only U and MAs in the multicomponent salt, which is attributed to the Gibbs energy differences among U, MAs, and REs. In addition, Simpson et al. [13] used gadolinium (Gd) metal to reduce chloride forms of U and magnesium (Mg) into their metallic forms. Approximately 90% of U and Mg elements were removed from the salt. This method is advantageous in terms of selective recovery among U/MA/RE elements; however, further investigations with respect to practical application in pyroprocessing need to be performed.

In this study, several RE metals were used to reduce UCl_3 and $MgCl_2$ (which served as a surrogate for $PuCl_3$) from the eutectic LiCl-KCl salt system that was enriched with $RECl_3$. Several experimental setups were used to give insights into the reaction yield and galvanic interaction between $RECl_3$ and UCl_3. In addition, different geometries of RE metals were applied to observe the formation and precipitation behavior of the reduced U. The results from this study will offer insights into the recovery of U via galvanic/chemical reactions with RE metals, which will be used to develop a process for purification of the ER salt via the selective recovery of U and actinide elements.

2. Experimental

Sample preparations and experiments were performed

Table 1. Summary of the experimental program for five experiments

Exp.	RE metals	Salt composition (wt%)						Mesh basket	Receiving crucible
		UCl_3	$MgCl_2$	$DyCl_3$	$CeCl_3$	$LaCl_3$	$NdCl_3$		
Run #1	La	3.3						SS	-
Run #2	Ce	0.66			0.6	0.86		-	Al_2O_3
Run #3	Ce	0.35					1.12	SS	SS
Run #4	Y	0.4		0.29	0.69			-	SS
Run #5	Y	0.5	0.31		1.05			-	SS

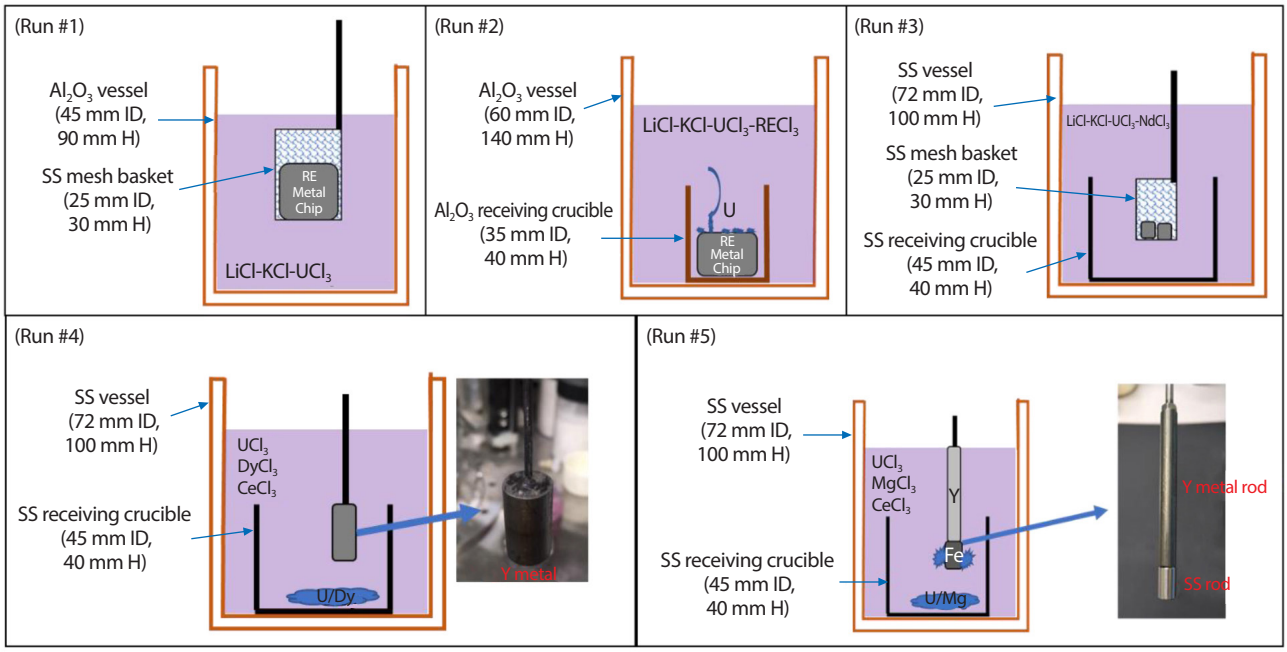

Fig. 1. Schematics of the experimental setup for each run.

inside a glovebox with a pure argon environment (≤ 10 ppm O_2 and H_2O). Anhydrous lithium–potassium chloride (LiCl -KCl, 99%) purchased from Sigma Aldrich was prepared in a vessel by removing possible moisture content at 523 K for 5 hours. UCl_3 (prepared via the reaction between U metal and $ZnCl_2$), $CeCl_3$, $LaCl_3$, $NdCl_3$, $DyCl_3$, and $MgCl_2$ (> 99.9%, Alfa Aesar for all five reagents) were used to prepare different compositions of the salt. Ce, Y, La metal rods (99.9%, Alfa Aesar) were used for the reduction of UCl_3.

In the present study, five experiments entailing different salt compositions were performed at 773 K whereby RE metals were introduced via different methods and geometries. Run #1 entailed the preparation of LiCl-KCl-3.3wt% UCl_3 in an Al_2O_3 vessel (45 mm in diameter and 90 mm in height). The La metal chips were loaded into a stainless-steel (SS) mesh basket (25 mm in diameter and 30 mm in height, 16 mesh) and lowered into the salt. Run #2 entailed the preparation of LiCl-KCl-UCl_3-$CeCl_3$-$LaCl_3$ in an Al_2O_3 vessel (60 mm in diameter and 140 mm in height). Ce metal chips were loaded into an Al_2O_3 crucible (35 mm in diameter and 40 mm in height). Run #3 was performed in the LiCl-KCl-UCl_3-$NdCl_3$ salt system with Ce metal chips in

Table 2. Summary of Gibbs free energies and standard potentials for actinides and rare earth elements [14-20]

Elements	ΔG_f ($kJ \cdot mol^{-1}$)	Standard potential (V vs. Cl_2/Cl^-)	Elements	ΔG_f ($kJ \cdot mol^{-1}$)	Standard potential (V vs. Cl_2/Cl^-)
UCl_3	-693.8	-2.49	$GdCl_3$	-815	-2.95
$NpCl_3$	-728.2	-2.67	YCl_3	-817.2	-3.07
$MgCl_2$	-778.5	-2.85	$NdCl_3$	-852	-3.08
$DyCl_3$	-783.2	-3.24 (at 723K)	$CeCl_3$	-863	-3.08
$PuCl_3$	-787.7	-2.78	$LaCl_3$	-880.8	-3.14
$AmCl_3$	-795.3	-2.84			

the SS mesh basket. In this experiment, the SS receiving crucible (45 mm in diameter and 40 mm in height) was placed at the bottom of the vessel to receive the reduced U metals. Run #4 was performed in the LiCl-KCl-UCl_3-$DyCl_3$-$CeCl_3$ salt system prepared in a SS vessel (72 mm in diameter and 100 mm in height). The Y metal rod was directly lowered into the salt by connecting with a SS rod, and the SS receiving crucible at the bottom was used. Run #5 involved the preparation of LiCl-KCl-UCl_3-$MgCl_2$-$CeCl_3$ salt in the SS vessel. The Y metal rod connected with the SS rod at the bottom was immersed in the salt. The SS receiving crucible was also used at the bottom. Figure 1 shows the schematics of the five experimental setups and Table 1 summarizes the experimental program for each run.

3. Theory

Table 2 lists the Gibbs free energy for the formation (ΔG_f) and standard reduction potential (E^0) for actinide and RE elements reported by various literature studies [14-20]. The values of ΔG_f for RE elements are more negative compared to those for actinides, indicating that the chloride formation of RE elements is relatively favorable. The present work used the difference between the ΔG_f values of actinide and RE elements to selectively recover actinide elements in the eutectic LiCl-KCl salt. The equations for the reaction can be expressed as.

$$RE + UCl_3 \rightarrow RECl_3 + U$$
(ΔG = -121 ~ 169 $kJ \cdot mol^{-1}$ at 773 K)

$$RE + MACl_3 \rightarrow RECl_3 + MA$$
(ΔG = -28 ~ -93 $kJ \cdot mol^{-1}$ at 773 K)

Similarly, galvanic interaction can be developed by driving an electric current between two or more metals with different electrode potentials. One metal acts as the cathode to gain electrons and the other as the anode to lose electrons. The potential difference between reactions at the two electrodes can be a driving force for the galvanic reaction. When RE metals are loaded in a SS mesh basket and lowered into the LiCl-KCl-$MACl_3$ salt system, there must be a galvanic interaction between RE metals and the SS basket as shown in the following reactions.

$U^{3+} + 3e^- \rightarrow U$ on SS basket
$MA^{3+} + 3e^- \rightarrow MA$
$RE \rightarrow RE^{3+} + 3e^-$ on RE metal

Based on the thermodynamic values listed in Table 2, the U^{3+}/U reaction is expected to occur more preferentially than other MA^{3+}/MA reactions in the galvanic reaction. $MgCl_2$ and $DyCl_3$ were used as $PuCl_3$ surrogate owing to the similarity between ΔG_f values. In the five experiments,

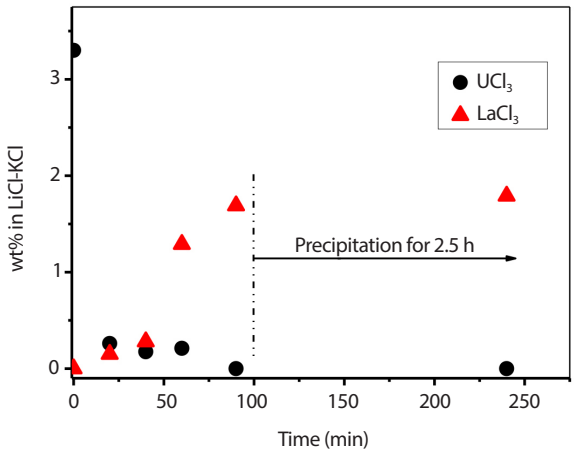

Fig. 2. Plots for UCl_3 and $LaCl_3$ concentration in Run #1.

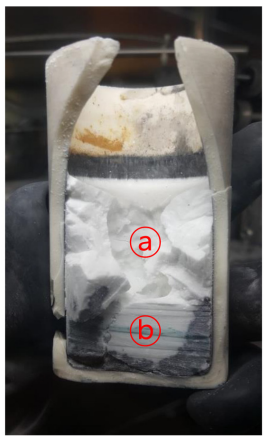

Fig. 3. Cross-section of the Al_2O_3 vessel after Run #1.

salt samples were taken with gentle agitations and analyzed using ICP-OES (Perkin-Elmer Optima 7300DV).

4. Results and Discussion

Run #1 involved immersion of La metal chips in the LiCl-KCl-3.3wt% UCl_3 salt system to observe the characteristics of U recovery and precipitation at the bottom of the Al_2O_3 vessel at 773 K. The La chips were loaded into the mesh basket to generate the galvanic interaction along with the chemical reaction. During the experiment, the reduced U was observed outside the mesh basket. The U was

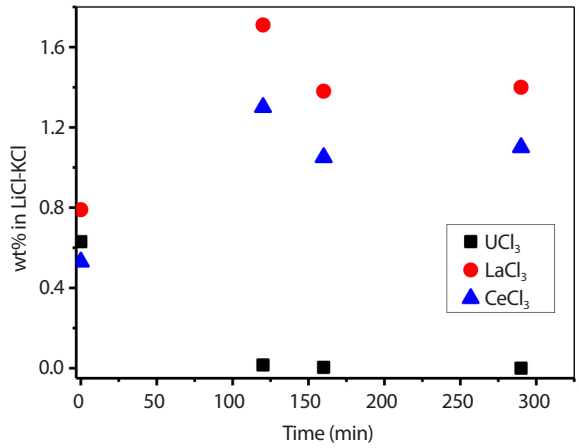

Fig. 4. Plots for UCl_3, $LaCl_3$, and $CeCl_3$ in the salt during Run #2.

deposited as a chunk powder that was easily detached via a little shake. The reaction lasted 2.5 h and salt samples were obtained to monitor salt composition. After the reaction was completed, the vessel was maintained in the furnace for another 2.5 h to allow the reduced U powder to settle at the bottom of the vessel. Figure 2 shows the concentration profiles for UCl_3 and $LaCl_3$ in the salt during Run #1 experiment. The UCl_3 concentration sharply dropped at the beginning of the run and was not detectable after 1.5 h of the reaction while the $LaCl_3$ concentration was increased to up to 1.7wt% in the salt. After the Run #1 experiment, the vessel was vertically cut for visual observation as shown in Fig. 3. The reduced U powder was settled and collected at the edge of the vessel bottom because the U powder formed outside the mesh basket sunk to the bottom. In addition, the salt samples obtained at different heights on the surface (see the position ⓐ and ⓑ in Fig. 3) exhibited no UCl_3 concentration indicating that the reduced U particle was completely precipitated at the bottom of the vessel.

Run #2 entailed the preparation of the LiCl-KCl-UCl_3-$LaCl_3$-$CeCl_3$ salt system at 773 K and Ce metal chips were used in an Al_2O_3 receiving crucible to reduce UCl_3 via a chemical reaction. The salt composition changes during Run #2 are shown in Fig. 4 depicting that UCl_3 concentration was lowered below 100 ppm after 2.5 h. The recovery rate of the reaction was considerably slower than that

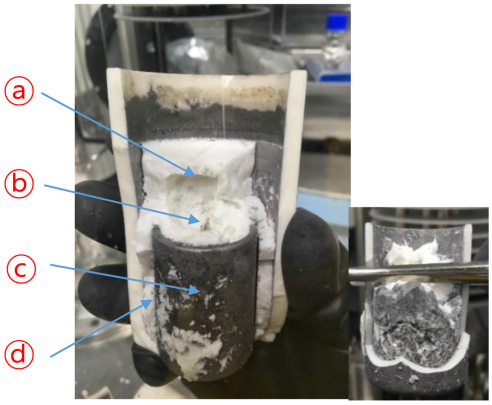

Fig. 5. Cross-sections of the Al_2O_3 vessel and receiving crucible in Run #2.

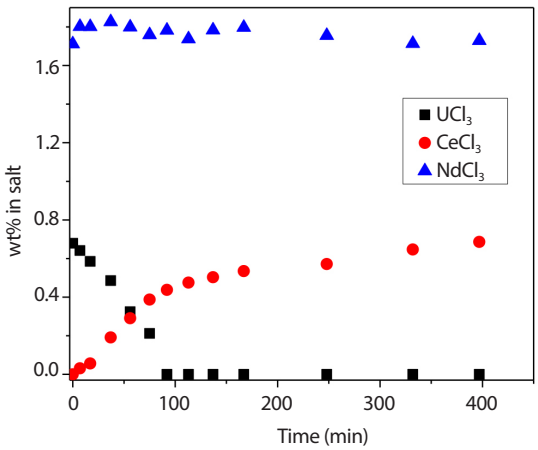

Fig. 6. Plots for concentrations of UCl_3, $CeCl_3$, and $NdCl_3$ in Run #3.

of both chemical and galvanic reactions. It can be postulated that the effective surface area of Ce metals was relatively smaller than that in the SS mesh basket. In addition, the diffusion of UCl_3 from bulk salt may be interfered with by the receiving crucible wall and the formed U powders around Ce metals in the receiving crucible. Compared to Run #1, the mesh structure was not used; therefore, any physical agitation was not conducted, which may affect the slow reaction or salt homogeneity. After the Run #2 experiment was completed, the Al_2O_3 vessel was cut vertically (see Fig. 5) showing that the recovered U powder was contained in the receiving crucible along with the unreacted Ce metals. The U concentration was not detected in the salt

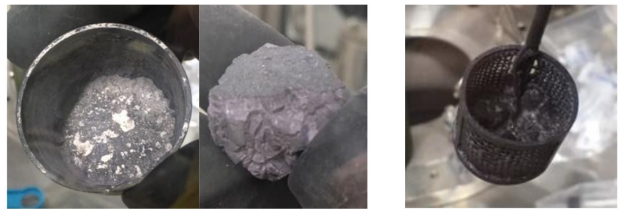

(a) (b)

Fig. 7. (a) The SS receiving crucible with collected materials and (b) the mesh basket after Run #3.

region (on the position ⓐ-ⓓ in Fig. 5). The Al_2O_3 receiving crucible and vessel were turned black and covered with black particles on the surface. ICP-OES read U content in the particles and the reaction mechanism was confirmed using HSC chemistry. Ce_2O_3 can be formed by the reaction between Ce metals and the Al_2O_3 crucible wall, which can react with UCl_3 again in the bulk salt as expressed in Eqs. (1) and (2). The results from Run #2 imply that the U particles can be formed outside the receiving crucible because the RE metals are reactive with the oxide-based ceramic crucible.

$$Ce + Al_2O_3 = Ce_2O_3 + Al$$
$$(G = -155\ kJ{\cdot}mol^{-1}\ at\ 773\ K) \quad (1)$$

$$Ce_2O_3 + UCl_3 = UO_2 + UO + CeCl_3$$
$$(G = -179\ kJ{\cdot}mol^{-1}\ at\ 773\ K) \quad (2)$$

Run #3 used the SS vessel and receiving crucible to inhibit the reaction between RE metals and the crucible. The LiCl-KCl-UCl_3-$NdCl_3$ salt system was prepared and Ce metals were placed in the mesh basket above the receiving crucible. During the experiment, the mesh basket was gently shaken to detach the recovered U powder onto the basket surface. Fig. 6 plots the salt composition during Run #3. The UCl_3 concentration steadily decreased while the $CeCl_3$ concentration increased accordingly. The UCl_3 concentration was lowered below 100 ppm in 1.5 h after which it seized to be detectable. The $NdCl_3$ concentration remained constant during the experiment indicating that $NdCl_3$ was not involved in the reaction with Ce metals. After Run #4, the SS receiving crucible was gently removed from the salt which

Fig. 8. An image of the Y metal rod during Run #4. The U particles were piled at the point where the Y rod came into contact with the SS wire.

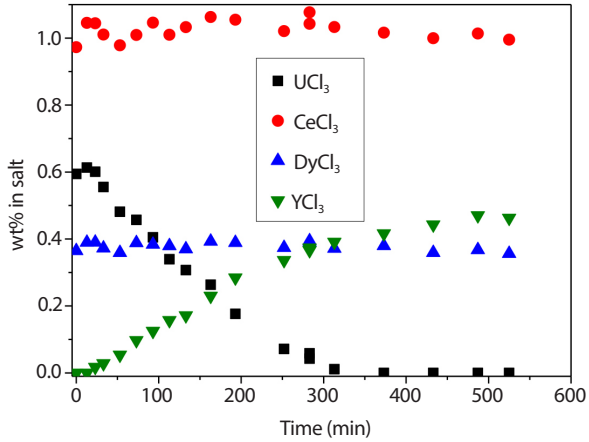

Fig. 9. The concentration plots for UCl_3, $CeCl_3$, $DyCl_3$, and YCl_3 during Run #4.

Fig. 10. The SS receiving crucible (left) and the collected materials was obtained at the bottom (right) after Run #4.

was cooled outside the furnace. When the SS receiving crucible cooled down, the salt was removed from the crucible and a thin layer of the recovered U powder was observed at the bottom as shown in Fig. 7(a). However, separation of the recovered powder from the salt was difficult. Figure 7(b) shows that the mesh basket contained a small portion of the recovered U powder despite the gentle shaking of the mesh basket. Significant reactions or oxidation was not observed on the SS crucible and vessel.

Run #4 introduced a Y metal rod in the LiCl-KCl-UCl_3-$DyCl_3$-$CeCl_3$ system. The Y metal rod was directly immersed in the salt via the connection with the SS wire (3 mm in diameter). Due to the direct exposure of the Y rod in the salt, facilitation of the chemical reaction without diffusion interruption by the container structure (wall of the receiving crucible) was expected. In addition, residual U powder was not expected on the Y rod compared to the experiments with the SS mesh basket that contained the remaining U powder. The $DyCl_3$ was used as a surrogate for $PuCl_3$ because the values of ΔG_f for $DyCl_3$ and $PuCl_3$ were similar. During Run #4, the Y rod was removed for visual observation as shown in Fig. 8. The surface of the Y rod was clean. However, deposited U particles were piled on the area where the rod came into contact with the SS wire for connection. The galvanic interaction can be considered to have happened at the connection between the Y rod and SS wire due to the potential difference that facilitates U reduction. The U powder was easily removed from the upper side when the Y rod was vertically vibrated. Figure 9 plots the composition changes for the elements during Run #4. UCl_3 concentration constantly decreased and reached below 100 ppm in 300 min while the YCl_3 concentration increased accordingly. The $CeCl_3$ concentration remained at approximately 1wt% during the reaction indicating that $CeCl_3$ did not react with the Y metal. However, the $DyCl_3$ concentration stayed at 0.4wt% and began to decrease very slowly when UCl_3 was almost depleted in the salt. It can be inferred that $DyCl_3$ was barely involved in the reaction in the beginning due to its very low activity coefficient; therefore, UCl_3 mainly reacted with the Y metal rod. When the reaction was completed, the SS receiving crucible was removed from the salt and cooled outside the furnace. The contents in the SS crucible, including the salt and recovered products, were collected as shown in Fig. 10.

Fig. 11. The collected product after the salt distillation operation in Run #4.

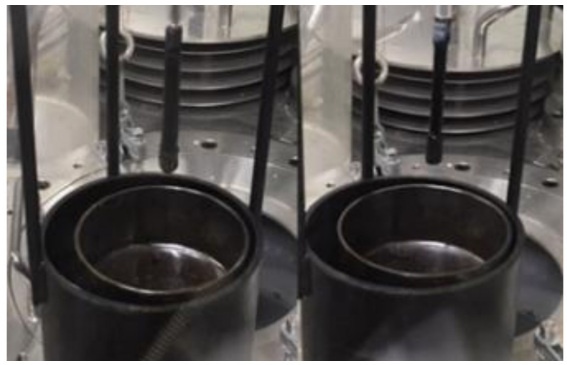

Fig. 12. Images of the Y rod during (left) and after (right) Run #5.

The collected materials were loaded in an Al_2O_3 crucible and distilled at a temperature of 1323 K and a pressure of 50 mTorr. Upon completion of the salt distillation, the dark powdery U product was obtained at the bottom of the crucible as shown in Fig. 11. The theoretical amount of recovered U was 1.658 g and the real amount recovered from the salt distillation was 1.47 g showing an 87% yield.

Previous runs, it was observed that the galvanic displacement was important to accelerate the reaction; however, it was difficult to control the reactive surface area for the galvanic reaction. Therefore, Run #5 introduced the SS rod (5 mm in diameter and 10 mm in length) contacted at the bottom of Y rod into the LiCl-KCl-UCl_3-$MgCl_2$-$CeCl_3$ salt system. The SS rod was prepared for the reactive surface area where the galvanic interaction was generated. As shown in Fig. 12 (left), U was mainly recovered on the surface of the SS rod, which was easily dropped into the SS receiving crucible via a gentle shake. At the end of the experiment, the reaction had made the Y rod distinctly thin (see Fig. 12 (right)). Figure 13 plots the concentrations of the elements in the salt during the experiment. The UCl_3 concentration quickly dropped below 100 ppm within 100 min of the reaction. By contrast, $MgCl_2$ concentration slowly decreased in the beginning; however, its reaction rate increased with the depletion of UCl_3 in the salt. This is because the U/U^{3+} reaction is more preferable than Mg/Mg^{2+} based on the value of ΔG_f; therefore, the recovered Mg metal reacts with UCl_3 again. The initial UCl_3 concentration rise in Run #4 and 5, which may be due

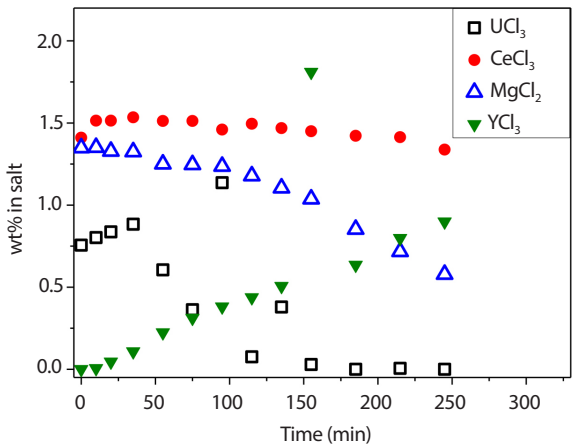

Fig. 13. Plots for UCl_3, $CeCl_3$, $MgCl_2$, and YCl_3 concentrations via Run #5.

to human errors on sample preparations and ICP analysis. Further experiments need to be conducted to elucidate U/Pu co-recovery using RE metals. Although the $CeCl_3$ concentration starts decreasing after the U depletion, the reaction rate of $CeCl_3$ with the Y rod was extremely slow.

5. Summary

In this study, the ER salt was simulated with high $RECl_3$ concentration and RE metals were introduced using several methods for the selective drawdown of the UCl_3 and $PuCl_3$ surrogate elements. Five experimental setups were used to understand the U recovery characteristics and behaviors of

Table 3. Comparison of the results from the five runs in the present work

Exp.	RE metal configuration	Reaction type	Reaction rate ($\times 10^5$ mol·min^{-1})	U/RE ratio in product
Run #1	La in Mesh basket	Galvanic reaction dominant	23	-
Run #2	Ce in Al_2O_3 receiving crucible	Chemical reaction dominant	1.9	-
Run #3	Ce in Mesh basket	Galvanic reaction dominant	22	11.1
Run #4	Y as a rod	Chemical reaction dominant	6.23	15
Run #5	Y rod contacted to a SS rod	Galvanic reaction dominant	16.6	7.3

the recovered U particle. It was confirmed that the introduced RE metals effectively reacted with UCl_3 in $RECl_3$ enriched salt systems; therefore, UCl_3 concentration can be lowered below 100 ppm. In addition, the recovered U particles were easily precipitated at the bottom and collected using a receiving crucible. In Run #1 and Run #2 experiments, RE metals were confirmed to react with the Al_2O_3 crucible, which caused UO_2 formation on the crucible wall via the mechanism expressed in Eqs. (1) and (2). In Run #3, the reduced U particle was successfully collected in an SS receiving crucible. However, separation of the reduced U particles from the salt was difficult. Run #4 introduced a Y metal rod directly into the salt to facilitate chemical reaction; however, galvanic interaction was also observed on the connection between the Y metal rod and the SS wire. The collected U particles at the bottom of the receiving crucible were loaded into an Al_2O_3 crucible for salt distillation. As a result, pure U element was obtained and the theoretical U recovery rate was confirmed to be 87%. In addition, $DyCl_3$ was implied to be an unsuitable surrogate material for $PuCl_3$ due to its low activity with RE metals. In Run #5, the SS rod was mounted under the Y rod to allow for galvanic interaction. The U particle was mainly deposited on the surface of the SS rod, which was easily detached via a little shake. In the present study, the galvanic interaction was generated along with the chemical reaction between $RECl_3$ and UCl_3 when the introduced RE metals came into contact with a metallic structure. The galvanic reaction appeared to be the dominant driving force over the chemical reaction to drawdown UCl_3 from the salt. A comparison among the five experiments (see Table 3) showed that the rate for UCl_3 removal was accelerated whenever a galvanic reaction occurred. However, a large amount of RE element was also co-recovered in the product with the galvanic reaction.

Acknowledgement

This study was supported by the National Research Foundation of Korea (NRF) grant funded by the Korean Ministry of Science, ICT (MIST) (grant number 2017M2A8A5015079).

.

REFERENCES

[1] M.F. Simpson and J.D. Law, Nuclear Fuel Reprocessing, Idaho National Laboratory Technical Report, INL/EXT-10-17753 (2010).

[2] International Atomic Energy Agency, Spent Fuel Reprocessing Options, IAEA Report, IAEA-TECDOC-1587 (2008).

[3] M. Iizuka, "Diffusion Coefficients of Cerium and Gadolinium in Molten LiCl-KCl", J. Electrochem. Soc., 145(1), 84-88 (1998).

[4] Z. Wang, D. Rappleye, and M.F. Simpson, "Voltammetric Analysis of Mixtures of Molten Eutectic LiCl-KCl Containing $LaCl_3$ and $ThCl_4$ for Concentration and Diffusion Coefficient Measurement", Electrochim. Acta,

191, 29-43 (2016).

[5] T. Murakami, A. Rodrigues, M. Ougier, M. Iizuka, T. Tsukada, and J-P. Glatz, "Actinides recovery from irradiated metallic fuel in LiCl-KCl melts", J. Nucl. Mater., 466, 502-508 (2015).

[6] S.X. Li, S.D. Herrmann, and M.F. Simpson, "Experimental Investigations into U/TRU Recovery Using a Liquid Cadmium Cathode and Salt Containing High Rare Earth Concentrations", Proc. of Global 2009, INL/CON-08-15166, September 6-10, 2009, Paris.

[7] M.F. Simpson, T. Yoo, D. Labrier, M. Lineberry, M. Shaltry, and S. Phongikaroon, "Selective Reduction of Active Metal Chlorides from Molten LiCl-KCl using Luthium drawdown", Nucl. Eng. Technol., 44(7), 767-772 (2012).

[8] M. Kurata, Y. Sakamura, T. Hijikata, and K. Kinoshita, "Distribution behavior of uranium, neptunium, rare-earth elements (Y, La, Ce, Nd, Sm, Eu, Gd) and alkaline-earth metals (Sr, Ba) between molten LiC1-KC1 eutectic salt and liquid cadmium or bismuth", J. Nucl. Mater., 227, 110-121 (1995).

[9] T. Kato, T. Inoue, T. Iwai, and Y. Arai, "Separation behaviors of actinides from rare-earths in molten salt electrorefining using saturated liquid cadmium cathode", J. Nucl. Mater., 357, 105-114 (2006).

[10] K. Uozumi, Y. Sakamura, K. Kinoshita, T. Hijikata, T. Inoue, and T. Koyama, "Development of Pyropartitioning Process to Recover Minor Actinide Elements from High Level Liquid Waste", Energy Procedia, 7, 437-443 (2011).

[11] H. Moritama, H. Yamana, S. Nishikawa, S. Shibata, N. Wakayama, Y. Miyashita, K. Moritani, and T. Mitsuhashira, "Thermodynamics of reductive extraction of actinides and lanthanides from molten chloride salt into liquid metal", J. Alloy. Compd., 271-273, 587-591 (1998).

[12] J.-B. Shim, T. Kim, G. Kim, S. Kim, S. Paek, D. Ahn, and S. Lee, "Uranium recovery tests using rare earth metals in LiCl-KCl molten salt", Proc. of Int. Pyroprocessing Research Conference, International Pyroprocessing Research Conference, September 21-23, 2016, Jeju.

[13] P. Bagri, C. Zhang, and M.F. Simpson, "Galvanic reduction of uranium (III) chloride from LiCl-KCl eutectic salt using gadolinium metal", J. Nucl. Mater., 493, 120-123 (2017).

[14] K. Fukasawa, A. Uehara, T. Nagai, N. Sato, T. Fujii, and H. Yamana, "Thermodynamic properties of trivalent lanthanide and actinide ionsin molten mixtures of LiCl and KCl", J. Nucl. Mater., 424, 17-22 (2012).

[15] J.J. Roy, L.F. Grantham, D.L. Grimmett, S.P. Fusselman, C.L. Krueger, T.S. Storvick, T. Inoue, Y. Sakamura, and N. Takahashi, "Thermodynamic Properties of U, Np, Pu, and Am in Molten LiCl-KCl Eutectic and Liquid Cadmium", J. Electrochem. Soc., 143(8), 2487-2492 (1996).

[16] K.C. Marsden and B. Pesic, "Evaluation of the Electrochemical Behaviors of $CeCl_3$ in Molten LiCl-KCl Eutectic Utilizing Metallic Ce as an Anode", J. Electrochem. Soc., 158(6), F111-F120 (2011).

[17] S.P. Fusselman, J.J. Roy, D.L. Grimmett, L.F. Grantham, C.L. Krueger, C.R. Nabelek, T.S. Storvick, T. Inoue, T. Hijikata, K. Kinoshita, Y. Sakamura, K. Uozumi, T. Kawai, and N. Takahashi, "Thermodynamic Properties for Rare Earths and Americium in Pyropartitioning Process Solvents", J. Electrochem. Soc., 146(7), 2573-2580 (1999).

[18] H. Tang, Y.D. Yan, M.L. Zhang, Y. Xue, Z.J. Zhang, W.C. Du, and H. He, "Electrochemistry of $MgCl_2$ in LiCl-KCl Eutectic Melts", Acta Phys.-Chim. Sinica, 29(8), 1698-1704 (2013).

[19] Y. Castrillejo, M.R. Bermejo, A.I. Barrado, R. Pardo, E. Barrado, and A.M. Martınez, "Electrochemical behaviour of dysprosium in the eutectic LiCl–KCl at W and Al electrodes", Electrochim. Acta, 50, 2047-2057 (2005).

[20] I. Barin, Thermochemical Data of Pure Substances, 3rd ed., Wiley-VCH Verlag GmbH, New York (1995).